# A Climatological Study of Vertical Transports by Cumulus-Scale Convection

ROBERT A. HOUZE, JR.[1]

*Dept. of Meteorology, Massachusetts Institute of Technology, Cambridge 02139*

(Manuscript received 3 July 1972, in revised form 26 April 1973)

ABSTRACT

Cumulus-scale vertical transports of sensible heat and angular momentum are computed by a technique which uses detailed precipitation measurements as basic input. Data from Boston, Mass., New Orleans, La., San Juan, P. R., and Tatoosh, Wash., are included in the study, and calculations are made for January, April, July and October. The seasonal and regional variations of the computed transports are consistent with climatology. The cumulus-scale transports are compared with the mean meridional, the synoptic-scale, and the total required eddy fluxes of heat and momentum, and are found to be of the same order of magnitude as the most important components of larger scale vertical flux during at least one season at each station.

## 1. Introduction

The study of atmospheric budgets of heat and angular momentum has provided much of our present understanding of the general circulation. Observational studies, such as those of Starr and White (1954), have shown that horizontal transports of these quantities are carried out by synoptic-scale eddies and to a certain extent by the mean meridional circulation. Vertical transports are not as well understood, largely because of difficulties in measuring vertical velocities on various scales. Investigations of upward fluxes have been restricted to techniques not involving direct measurements of the vertical motions. The amounts of heat and momentum transported upward by the mean meridional circulation have been estimated with vertical velocities deduced from mass continuity and observed horizontal winds (e.g., Palmén and Newton, 1969). Numerical simulations of the general circulation, such as those of Smagorinsky *et al.* (1965) and Manabe *et al.* (1970), have provided estimates of synoptic-scale vertical fluxes. The effect of cumulus-scale convection has been an especially elusive aspect of the general circulation. The small horizontal dimensions and transient nature of individual cumuli make it practically impossible to measure directly with any completeness the amount or physical properties of air transported vertically.

Austin and Houze (1973) describe an indirect method for computing cumulus-scale transports in which the basic premise is that the net amount of air transported upward within precipitating cumulus cells can be deduced from observed rainfall amounts. In the present paper, their technique is applied in a climatological study of vertical transports of sensible heat and angular momentum. Transports by precipitating cumuli are computed for four stations representing widely varying climates. The magnitudes of the cumulus transports are compared with those of larger scale fluxes, and some insight is thus gained into the relative importance of cumulus-scale convection as a transport mechanism.

[1] Present affiliation: Department of Atmospheric Sciences, University of Washington, Seattle.

## 2. Model for computing transports

The method for computing cumulus transports is described by Austin and Houze (1973; hereafter referred to as AH) and is not repeated here, except for additions and details which are pertinent to this particular study.

The basic data are rain gauge records. A *storm* is defined as a continuous period of precipitation at a station and calculations of transports are made for individual storms on an hour-by-hour basis, then summed over seasonal periods at different stations. Each storm is composed of cumulus-scale showers, or *cells*, which are located within *mesoscale* areas of lighter rain. The mesoscale areas may in turn be located within *synoptic-scale* regions of still less intense precipitation.

The following quantities are considered given or observed in the calculations. Symbols with the subscript $n$ refer to a particular hour during the storm while those without this subscript are either storm totals or storm averages.

$(\Delta t_c)_n$, $(\Delta t_m)_n$, $(\Delta t_s)_n$ time during hour $n$ when cells, mesoscale areas, and synoptic areas, respectively, are over the rain gauge

$(R_c)_n$, $(R_m)_n$, $(R_s)_n$ cellular, mesoscale and synoptic rainfall amounts for hour $n$ of the storm

$(u_e)_n$ westerly wind speed outside of cells during hour $n$

| | |
|---|---|
| $T_c$ | temperature in cells representing average conditions during storm |
| $q_0$ | water vapor mixing ratio outside storm |
| $z_B$, $z_T$, $z_P$ | average heights of cell bases, cell tops, and top of non-cellular precipitation for storm. |

The model-storm quantities which are computed from the various observed parameters include:

| | | |
|---|---|---|
| $C$ | water condensed in cells | |
| $M_c$ | mass of air transported upward within cumulus cells | for the rain which falls on a unit area during storm |
| $M_m$ | mass of air transported upward within mesoscale areas | for the rain which falls on a unit area during storm |
| $M_s$ | mass of air transported upward within synoptic areas | for the rain which falls on a unit area during storm |
| $(u_c-u_e)_n$ | westerly wind speed difference between air inside and outside cells during hour $n$ | |
| $T_c-T_e$ | temperature difference between air inside and outside cells, average conditions for storms | |
| $\tau_{sh}$ | sensible heat transport due to air rising in cumulus scale cells | |
| $\tau_{am}$ | angular momentum transport due to air rising in cumulus-scale cells. | |

All of these quantities are functions of height. The last two, $\tau_{sh}$ and $\tau_{am}$, are the transports which are analyzed climatologically.

The equation for $C$ is

$$C=\beta(R_c+\alpha R_m-R_A-R_B), \quad (1)$$

where $R_A$ and $R_B$ are any components of $R_c$ produced directly above and below the cells by larger scale lifting, $\alpha$ is the fraction of mesoscale precipitation which was condensed in cellular updrafts, and $\beta$ represents the ratio of $C$ to the total precipitation of cellular origin.

Vertical mass transports in the cells, mesoscale areas and synoptic-scale areas are related to precipitation amounts and condensation by the following equations, which express the conservation of water in each portion of the storm:

$$C=\int_{z_B}^{z_T} M_c\left[\frac{1}{M_c}\left(\frac{dM_c}{dz}\right)_\epsilon (q_e-q_c)-\frac{dq_c}{dz}\right]dz, \quad (2)$$

where $M_c^{-1}(dM_c/dz)_\epsilon$ is the entrainment rate and $(q_e-q_c)$ is the difference in mixing ratio between the entrained air and that in the cells;

$$(1-\alpha)R_m=\int_0^{z_P}\left\{(q_s-q_m)\left(\frac{dM_m}{dz}+\frac{dM_c}{dz}\right)\delta-M_m\frac{dq_m}{dz}\right.$$
$$\left.+(q_c-q_m)\left[\left(\frac{dM_c}{dz}\right)_\epsilon-\frac{dM_c}{dz}\right]\right\}dz, \quad (3)$$

and

$$R_s=\int_0^{z_P}\left[(q_0-q_s)\left(\frac{dM_s}{dz}+\frac{dM_m}{dz}\right)\delta-\frac{dq_s}{dz}M_s\right]dz, \quad (4)$$

where $q_s$ and $q_m$ are the water vapor mixing ratios in the synoptic and mesoscale areas, respectively, and $\delta$ is unity for $z<\zeta$ and zero otherwise.

The mass transport terms $M_c$, $M_m$ and $M_s$ are all assumed to have maxima at the same level $\zeta$ and to decrease monotonically above and below. The profile of $M_c$ and the entrainment rate are specified as in AH (Section 6). The mesoscale and synoptic-scale transports $M_m$ and $M_s$ simply decrease parabolically to zero at the surface and at the top of the model storm which is at $z_T$ or 10 km whichever is higher. The temperature in the mesoscale and synoptic-scale precipitation areas at any level is taken to be that of the general environment, and the air in all precipitation areas is assumed to be saturated.

The value of $M_c$ at cell top is specified as

$$M_c(z_T)=\frac{\Delta t_c}{\Delta t_m}M_m(z_T), \quad (5)$$

reflecting the assumption that at level $z_T$ lifting in the cells is the same as in the surrounding mesoscale areas. The typically small quantities $R_A$ and $R_B$ are given by

$$R_A=\begin{cases}\displaystyle\int_{z_T}^{z_P}\frac{\Delta t_c}{\Delta t_m}M_m\left(-\frac{dq_m}{dz}\right)dz, & z_T<z_P\\ 0, & z_T>z_P\end{cases} \quad (6)$$

$$R_B=\int_0^{z_B}\frac{\Delta t_c}{\Delta t_m}M_m\left(-\frac{dq_m}{dz}\right)dz. \quad (7)$$

Eqs. (1)–(7) are solved simultaneously with the expressions for $(T_c-T_e)$ and $(u_e-u_c)$ which are given in Sections 7 and 8 of AH. The transports of sensible heat and angular momentum by cumulus updrafts are then calculated from

$$\tau_{sh}(z)=M_c(z)c_p[T_c(z)-T_e(z)], \quad (8)$$

$$\tau_{am}(z)=a\cos\phi\sum_n [M_c(z)]_n[u_c(z)-u_e(z)]_n, \quad (9)$$

where $c_p$ is the specific heat of air at constant pressure, $a$ the earth's mean radius, and $\phi$ the latitude of the station. As in AH, transports computed from (8) and (9) may be expected to underestimate actual transports because effects of downdrafts are not included. In the model, the temperature difference between cells and environment depends primarily on cell depth which does not vary much within the course of a storm. Thus, $\tau_{sh}$ is computed from storm-averaged conditions. Environmental wind shear, on the other hand, may vary considerably from one hour to the next. Angular mo-

TABLE 1. Extent of data sample.

| Station | Number of storms* | Number of hours | Periods covered |
|---|---|---|---|
| Boston, Mass. | 139 | 1066 | Jan–Dec 1962, 1963, 1969<br>Jan–Feb 1966, 1967 |
| New Orleans, La. | 30 | 166 | Jan 1966, Apr 1964,<br>Jul 1963, Oct 1962 |
| San Juan, P.R. | 125 | 207 | Jan 1962, Apr 1964,<br>Jul 1964, Oct 1966 |
| Tatoosh, Wash. | 62 | 453 | Jan 1964, Apr 1962,<br>Jul 1964, Oct 1963 |

* The term storm refers to a period of precipitation at a station.

mentum transports for a storm are therefore computed for each hour and summed. Vertical mass transport in cells is apportioned to individual hours in the same ratio as the measured cellular rain, i.e.,

$$(M_c)_n = \frac{(R_c)_n}{R_c} M_c. \tag{10}$$

For each storm, computations of $\tau_{sh}$ and $\tau_{am}$ are made for a number of combinations of the parameters $\alpha$ and $\beta$ with $\alpha$ ranging from 0 to 1 and $\beta$ from 1 to 3.

## 3. Selection of parameters for best estimate and upper and lower limits

The combination of $\alpha$ and $\beta$ which gives the most realistic estimate of cellular condensate $C$ and the associated cellular lifting, varies from storm to storm. In AH it is concluded from empirical evidence and physical reasoning that the best estimate for $C$ (excluding any condensate which is re-evaporated in the downdraft) is $3R_c$, and the minimum value is $R_c$. In this paper an upper limit for the transports is determined by considering reasonable constraints on model lifting.

The quantities

$$W^* = \frac{M_c(\zeta)}{\rho(\zeta)\Delta t_c}, \tag{11}$$

$$\bar{W} = \frac{M_c(\zeta)+M_m(\zeta)+M_s(\zeta)}{\rho(\zeta)(\Delta t_c+\Delta t_m+\Delta t_s)}, \tag{12}$$

where $\rho$ is the density of air, are computed to give a rough estimate of the average vertical velocity at level $\zeta$ for the cells ($W^*$) and for the storm as a whole ($\bar{W}$). For each storm $W^*$ is compared with the vertical velocities in Table 1 of AH. Any combination of $\alpha$ and $\beta$ for which $W^*$ exceeds the corresponding value in the table by as much as 2 m sec$^{-1}$ is considered to give an unrealistically large value for $M_c$.

For selected storms $\bar{W}$ was compared with a vertical velocity calculated from observed horizontal winds. The comparisons which were made are discussed in the Appendix. It was found that in storms of synoptic-scale dimensions the model overestimated the storm-average vertical velocity for combinations of large $\alpha$ with $\beta > 1$. This result is expected if condensate left aloft by cumulus updrafts is rained out within the larger scale storm. Therefore, in widespread storms, defined as those taking longer than 4 hr to pass over the rain gauge, only combinations of $\alpha$ with $\beta = 1$ are considered reasonable.

For each storm the combination of $\alpha$ and $\beta$ which yielded the largest value for $M_c$ while remaining within the imposed constraints was selected to provide the upper limit for the computed transports. The combination which resulted in the closest approximation to $C = 3R_c$, while still remaining within the constraints, was selected for the best estimate. For the lower limit the values $\alpha = 0$, $\beta = 1$ were used.

## 4. Data

The climatological analysis of the cumulus transports was based on data from four stations. Table 1 lists the number of storms, the total hours of precipitation, and the time periods included for each station. The types of data used are summarized in Table 2.

In most of the situations covered, the model appears to be applicable. At San Juan, cells were occasionally isolated rather than being embedded in mesoscale rain areas. Since these cells were weak and shallow and contributed only slightly to transports computed over climatological time periods, the model was not altered and they were treated as if they had a saturated environment.

## 5. Data handling

### a. *Input parameters*

For the quantities listed as observed in Section 2 which are functions of height, idealized profiles are assumed, with numerical values selected to provide best fit with available sounding data. The cellular temperature $T_c$ is assumed to follow the moist adiabat corresponding to the mean equivalent potential temperature $\theta_E$ in the environment. The westerly wind speed $(u_e)_n$ is approximated with a linear distribution given by its slope, or shear, $(B)_n$, the values for each hour $n$ being interpolated between actual input shears $(B)_\sigma$ obtained at sounding times $\sigma$. The mixing ratio $q_0$ is obtained by multiplying the saturation mixing ratio $q_e$, which applies within the storm, by a relative humidity function representing average conditions outside the storms. The function used is illustrated in Fig. 1 of AH where $H_1$ is the mean relative humidity below some level $z^*$ and $H_2$ is the mean relative humidity above $z^*$. The parameters $H_1$, $z^*$ and $H_2$ are constant for a given storm but may vary from one storm to another.

Thus, the parameters actually serving as input for the computer program and the types of data from which

Table 2. Characteristics of data for each station in climatological sample.

| Station | Type of measurements | Frequency of measurements | Actual locations of instruments | Form of records | Organization from which records were obtained |
|---|---|---|---|---|---|
| Boston | Tipping-bucket rain gauges with sensitivities ranging from one tip per 0.01 mm to one tip per 0.6 mm of rain | Continuous | Cambridge and West Concord, Mass. | Timed strip charts with one mark for each tip | MIT |
| | Radar range-height indicator (RHI) | ½ to 1 hr intervals | Cambridge, Mass. | Photographs of RHI scope | MIT |
| | Rawinsonde | 12-hr intervals | Portland, Me. Albany, N. Y. Nantucket, Mass. | *Northern Hemisphere Data Tabulations* in book and microfilm form. Also punched cards WBAN Card Deck 645 | NOAA |
| New Orleans | Tipping-bucket rain gauges, one tip per 0.25 mm of rain | Continuous | New Orleans, La. | Microfilm of triple register strip charts | NOAA |
| | RHI | 1-hr intervals | New Orleans, La. | Written records from WBAN 60 | NOAA |
| | Rawinsonde | 12-hr intervals | Burrwood, La., before Aug. '65 Boothville, La., after Aug. '65 | Punched cards | NOAA |
| San Juan | Tipping-bucket rain gauges, one tip per 0.25 mm of rain | Continuous | San Juan, P. R. | Microfilm of triple register strip charts | NOAA |
| | RHI | 1-hr interval | Ramey AFB, P. R. | Written records on form WBAN 60 | NOAA |
| | Rawinsonde | 12-hr intervals | San Juan, P. R. | Punched cards | NOAA |
| Tatoosh | Tipping-bucket rain gauges, one tip per 0.25 mm of rain | Continuous | Tatoosh, Wash. | Microfilm of triple register strip charts | NOAA |
| | RHI* | | | | |
| | Rawinsonde | 12-hr intervals | Tatoosh, Wash. | Punched cards | NOAA |

* No records available, see text for discussion of assumptions.

they are obtained are:

| Input parameters | Type of data |
|---|---|
| $(R_c)_n$, $(R_m)_n$, $(R_s)_n$, $(\Delta t_c)_n$, $(\Delta t_m)_n$, $(\Delta t_s)_n$ | High-resolution rain gauge |
| $z_T$, $z_P$ | Radar range-height observations |
| $z_B$, $\theta_E$, $(B)_\sigma$, $H_1$, $H_2$, $z^*$ | Rawinsonde |

### b. *Precipitation amounts and times*

The input $R$'s and $\Delta t$'s are calculated as cumulative totals for each hour. Criteria consistent with the findings of Austin and Houze (1972) are used to determine when the areas of various scales are over the gauge. A cell is assumed to last 3 min and is associated with any peak in the rainfall trace for which the precipitation rate is at least 5 mm hr$^{-1}$ and at least twice as large as the minimum rainfall rate within $\pm 5$ min. In addition to cells identified by this criterion, any rain exceeding 20 mm hr$^{-1}$ in intensity is considered cellular. A mesoscale area is assumed to be over a gauge if the precipitation rate increases by a factor of 2 or more during a period of a few minutes then decreases again after a period of ¼ to 4 hr. In addition, any rain falling at a rate exceeding 4 mm hr$^{-1}$ is called mesoscale, unless a cell is over the gauge. Precipitation not considered cellular or mesoscale by any of the above criteria is called synoptic.

For Tatoosh, a simplified procedure was followed where no attempt was made to identify mesoscale rain. If precipitation was not cellular, it was designated synoptic.

### c. *Vertical precipitation structure*

The height $z_T$ of cellular precipitation is readily inferred from radar RHI data. However, $z_P$ is more difficult to determine since the non-cellular precipitation is much less intense and harder to detect. In a number of storms $z_P$ was assumed to be equal to $z_T$, which was usually more or less the case when observations were adequate to indicate its value.

The cell base $z_B$ cannot usually be determined with radar. Therefore, an average value of 1.0 km (0.5 km for San Juan) was assumed for most storms. If soundings indicated a strong warm-frontal inversion, $z_B$ was taken to be the top of the stable layer.

Records of the RHI were not available for Tatoosh, and a cell top of 6 km was used in all calculations for this station. This value is representative of the average conditions at Boston which, although of a different climate, is at approximately the same latitude as Tatoosh. Radar records were also not available for a few storms at Boston, and a seasonally averaged cell-top height was used.

*d. Temperatures, humidities and winds*

The equivalent potential temperature and the humidity parameters were determined visually from plotted soundings. The wind shear $(B)_\sigma$ was calculated as the slope of the least-square fit to the observed westerly winds for soundings taken before, during and after the passage of each storm.

## 6. Computed monthly transports

The storms in the data sample were grouped by station according to the month in which they occurred, regardless of the year. The cumulus-scale heat and angular momentum transports, $\tau_{sh}$ and $\tau_{am}$, were summed over all of the storms in each station-month category. Summations were done separately for heat and momentum and for lower limits, best estimates, and upper limits, so that six totals were computed for each month at a station. Each of the six totals was then normalized by the ratio of the climatologically averaged number of hours of precipitation[2] to the number of hours of precipitation sampled for the station and month under investigation, an hour of precipitation being defined as an hour during which at least 0.01 inch of precipitation was measured. The resulting curves represent the total cellular transport which would occur in a month with an average number of hours of precipitation. Since computations were made from rain gauge data, the transports are average values per square centimeter per month. The computed curves of monthly transport are shown for January, April, July and October for each station in Figs. 1–8. For Tatoosh only two curves are shown for each month since the rainfall data were processed in a simplified manner and only lower limits and best estimates were computed.

[2] The climatologically averaged number of hours of precipitation was obtained for different months and stations from the *Decennial Census of United States Climate—Summary of Hourly Observations*, published by the U.S. Weather Bureau. Ten-year statistics on the hourly occurrence of precipitation were not available for Tatoosh; data for Salem, Ore., were therefore substituted doubling the number of hours of rainfall in any given month at Salem to approximate the conditions at Tatoosh where the monthly rainfall amounts are approximately twice those at Salem.

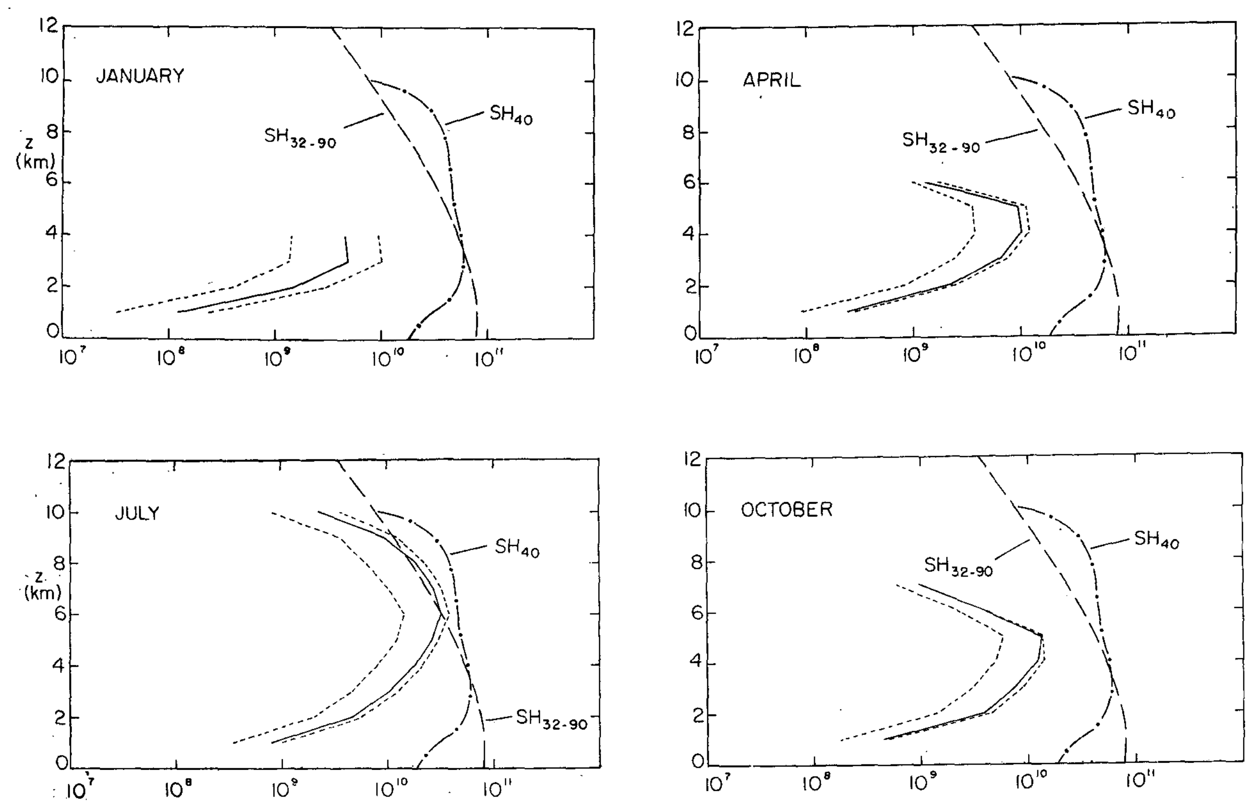


FIG. 1. Monthly values for upward transport of sensible heat by cumulus-scale cells at Boston. Solid curve is best estimate, while short-dash curves are for lower and upper limiting values of cellular condensation. $SH_\phi$ is synoptic-scale eddy flux of heat at latitude $\phi$ as computed by Manabe *et al.* (1970), and $SH_{\phi_1-\phi_2}$ is the total required upward flux of heat by eddies of all scales for latitude belt $\phi_1-\phi_2$ as computed by Palmén and Newton (1969). Units: ergs cm$^{-2}$ month$^{-1}$.

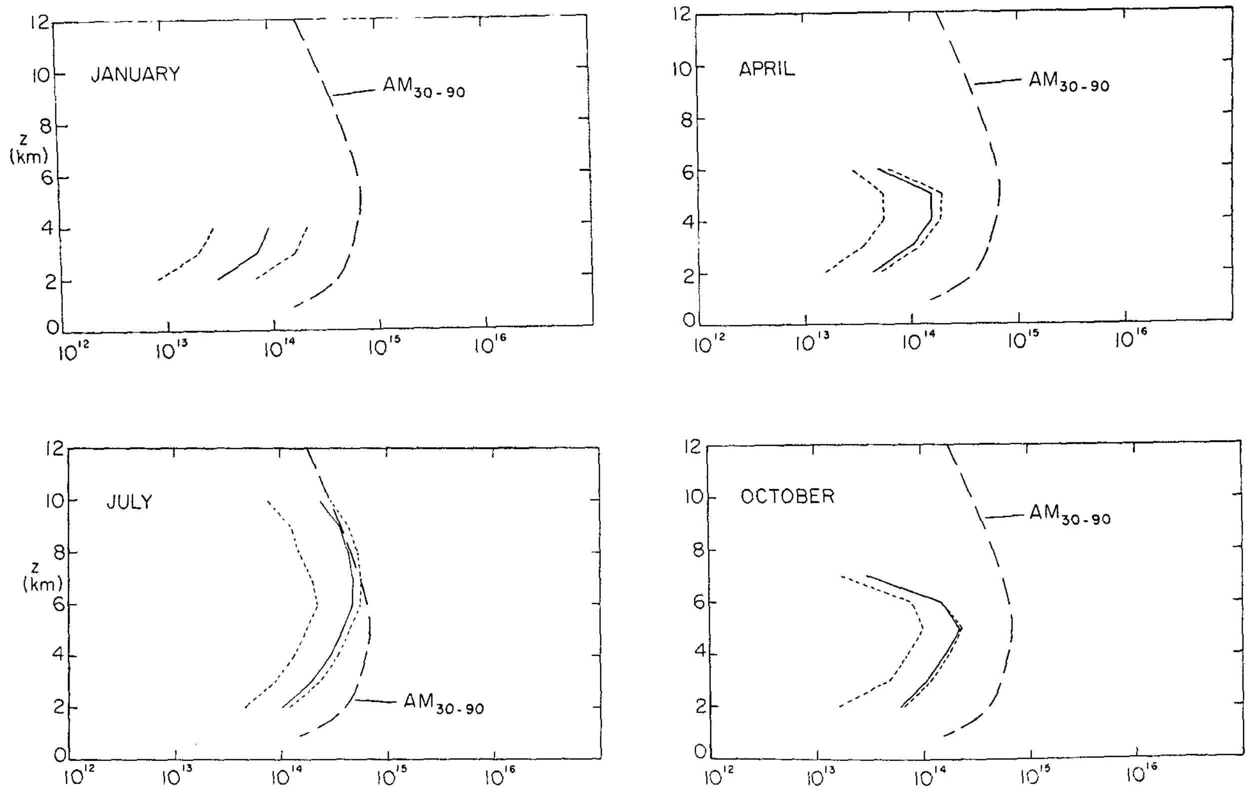


FIG. 2. Monthly values for downward transport of angular momentum by cumulus-scale cells at Boston. Solid curve is best estimate while short-dash curves are for lower and upper limiting values of cellular condensation determined from rainfall measurements. $AM_{\phi_1-\phi_2}$ is the average downward flux of angular momentum by the mean meridional circulation for latitude belt $\phi_1-\phi_2$ as computed by Palmén and Newton (1969). Units: gm sec$^{-1}$ month$^{-1}$.

The lower and upper limiting values shown in Figs. 1–6 represent the limits of uncertainty associated with relating condensation to precipitation. They have been evaluated storm-by-storm from constraints on model lifting and thus represent a further test of the reasoning given in AH (Section 5), where the uncertainty in the value of $C$ deduced from $R_c$ is estimated to be plus or minus a factor of 3. Figs. 1–6 also suggest that the upper limit is approximately ten times the lower limit, but the best estimate is generally considerably closer to the upper limit. Other uncertainties in the model are discussed in AH and an overall uncertainty of plus or minus a factor of 4 is estimated for the heat and momentum transports. It should again be recognized that neither the computations nor the estimates of uncertainty include effects of cellular downdrafts. Qualitatively, the effect would be to increase the heat and momentum transports especially in the lower portions of the cells. Instrumental errors and errors introduced by smoothing or idealizing input quantities might be considerable for a single datum. For example, at a given station and hour the assumed westerly wind component, which varies linearly with height and was obtained by interpolation between soundings at 12-hr intervals, might differ significantly from the actual wind profile; or in an individual cell the duration of cellular rainfall may not be exactly 3 min. However, smoothing has been done around average values and many storms have been sampled so that there should be no consistent bias. The errors tend to cancel each other and should not significantly affect the average computed monthly transports.

## 7. Seasonal and geographical variations

The regional and seasonal variations of the monthly transports in Figs. 1–8 are consistent with the climatology of convective activity. The magnitude and vertical extent of the transports are highly correlated with the proximity of the station to sources of unstable maritime tropical air. For example, the transports at San Juan (Figs. 6 and 7) are largest during summer and fall when this station is located on the southwest of the Atlantic subtropical anticyclone. Comparison of the results for New Orleans and Boston (Figs. 1–4) shows decreasing transports as the position of the station becomes farther to the west and north around the perimeter of the subtropical high. The seasonal variation of the vertical transports at Boston reflects the stronger and deeper convection of summer thunderstorms as compared with the smaller cells embedded in winter cyclones.

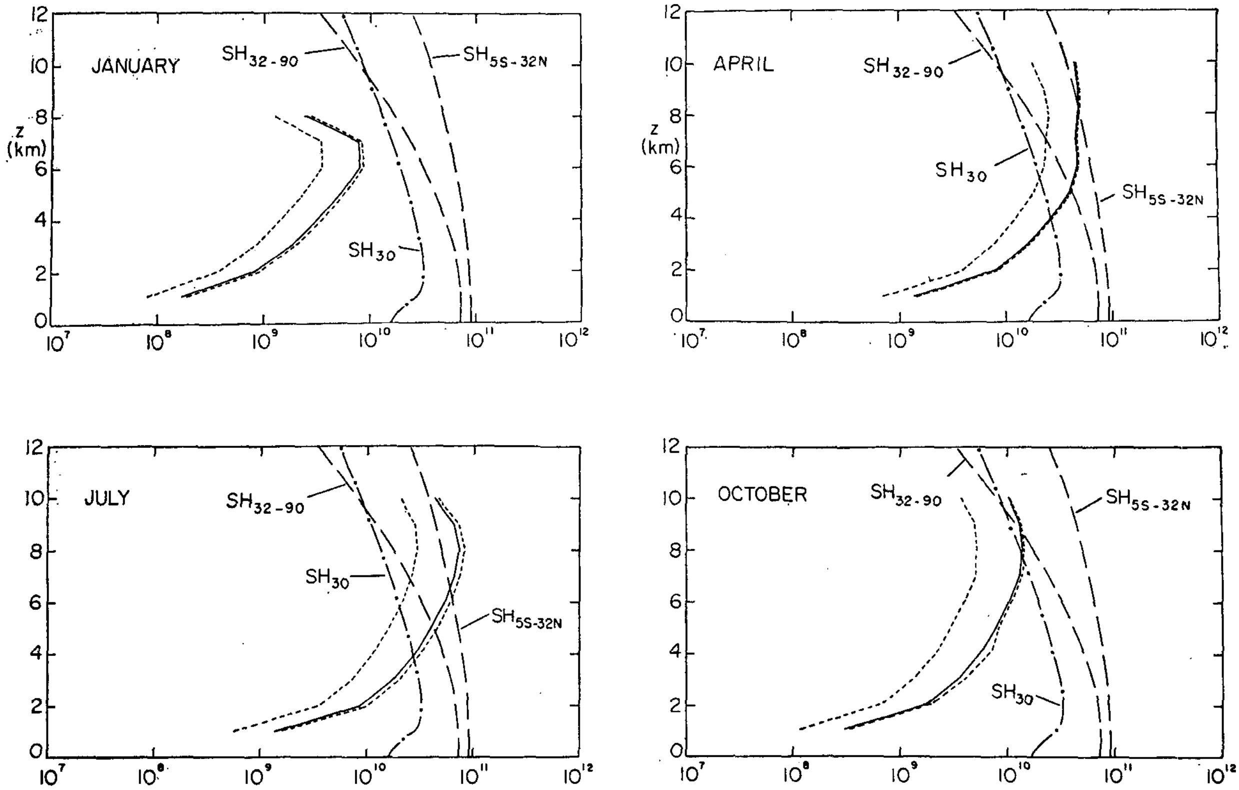


FIG. 3. Monthly values for upward transports of sensible heat at New Orleans. Notation as in Fig. 1.

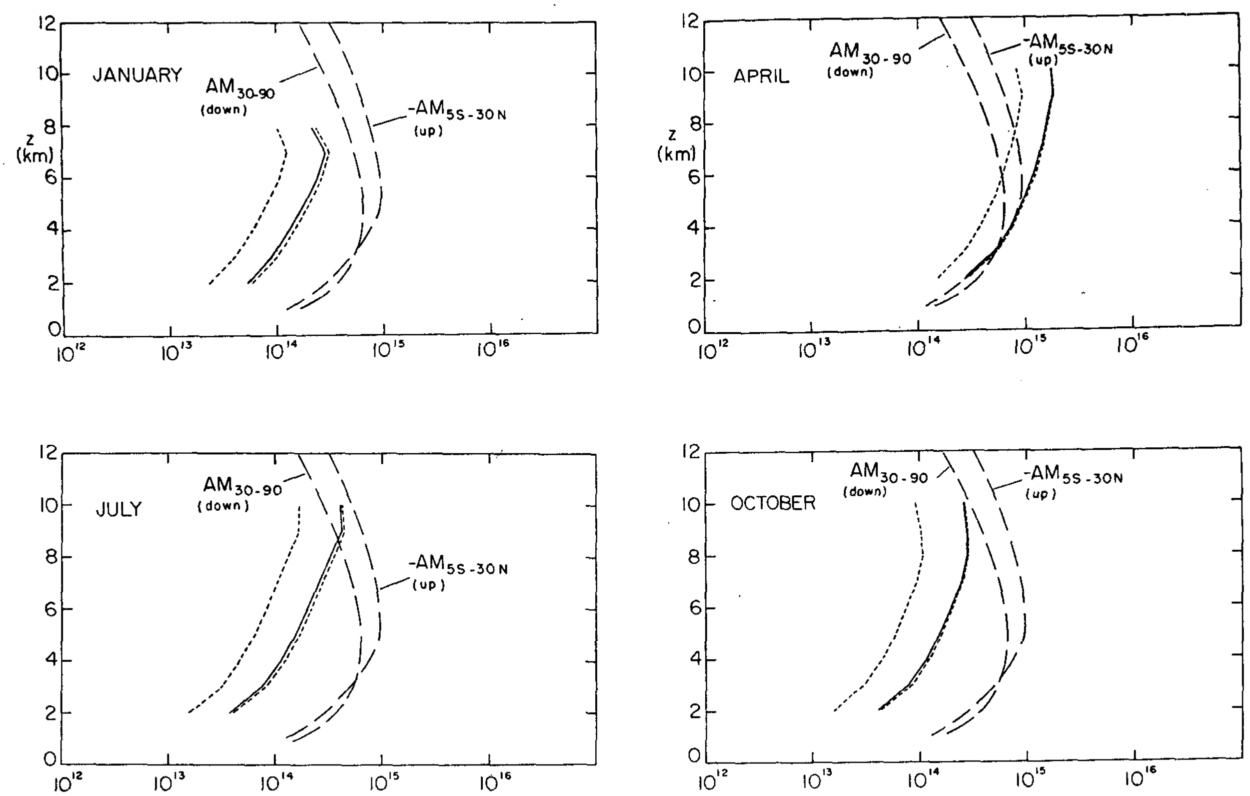


FIG. 4. Monthly values for downward transport of angular momentum by cumulus-scale cells at New Orleans. Notation as in Fig. 2.

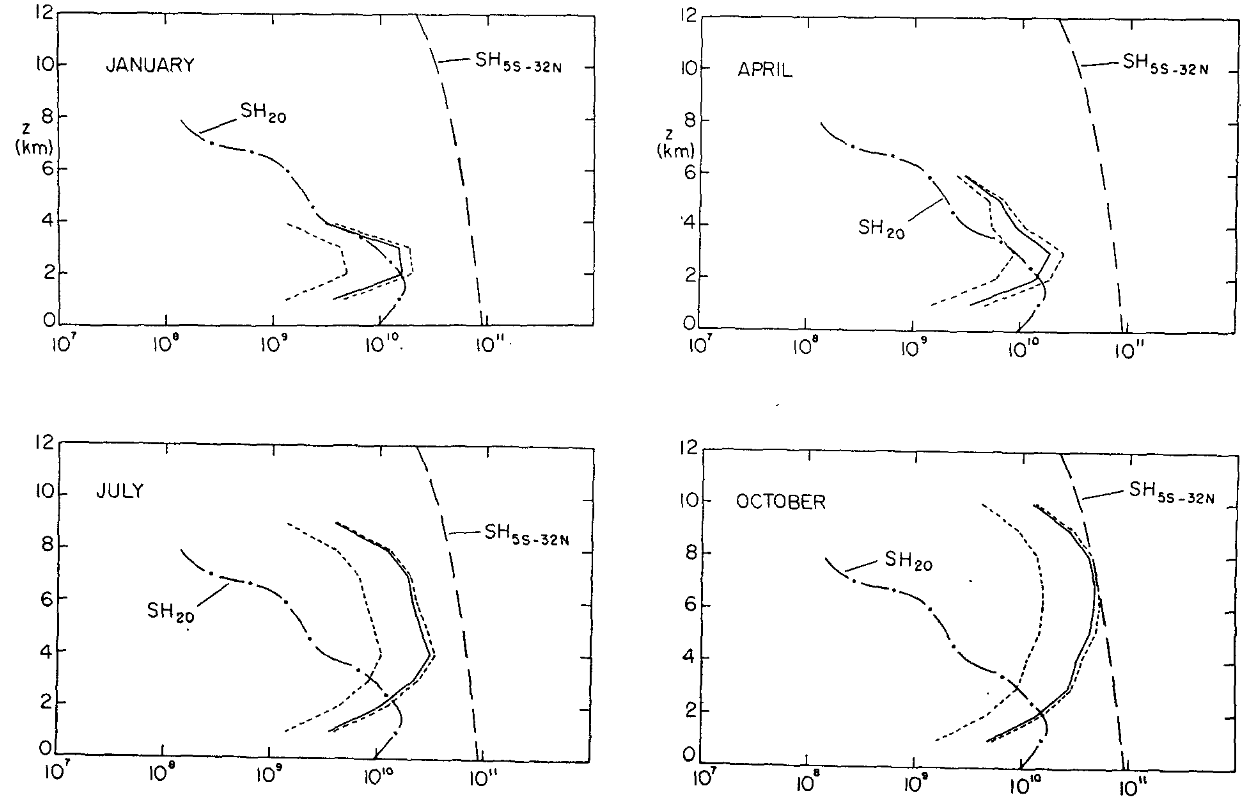


FIG. 5. Monthly values for upward transport of sensible heat at San Juan. Notation as in Fig. 1.

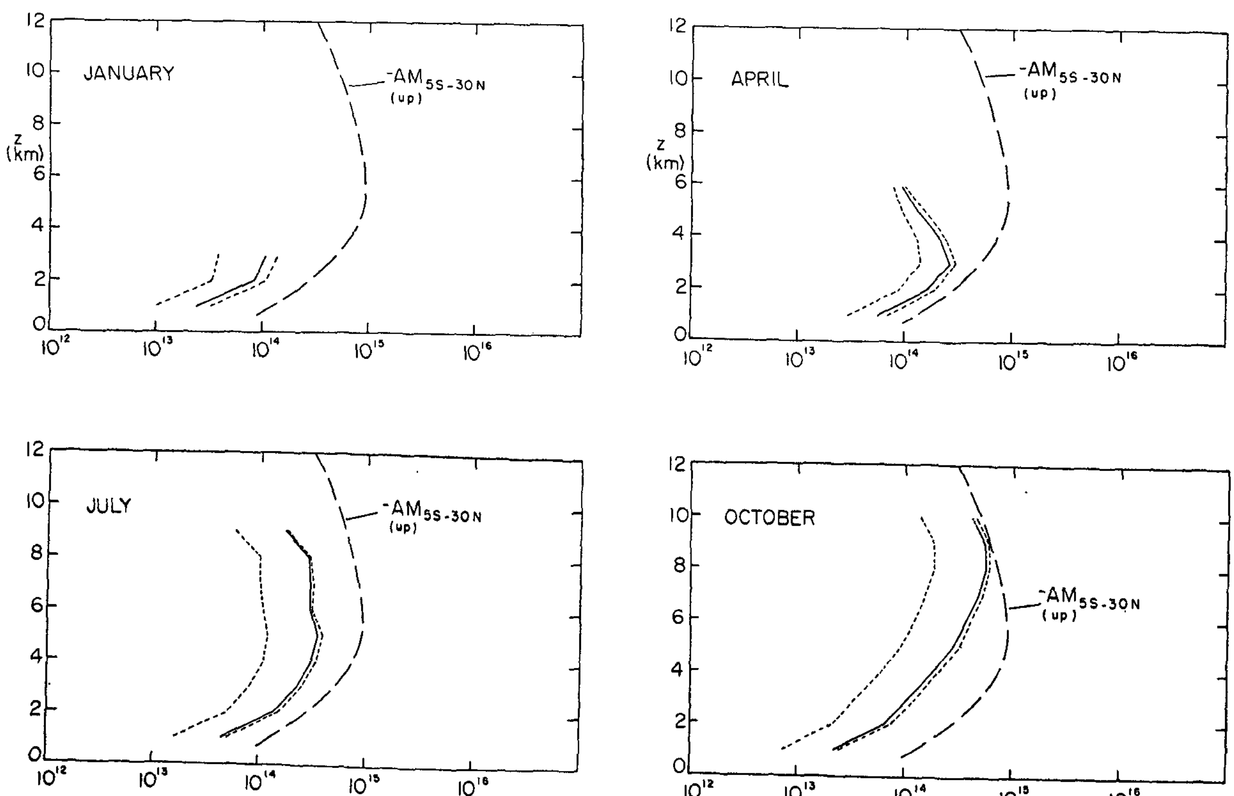


FIG. 6. Monthly values for downward transport of angular momentum by cumulus-scale cells at San Juan. Notation as in Fig. 2.

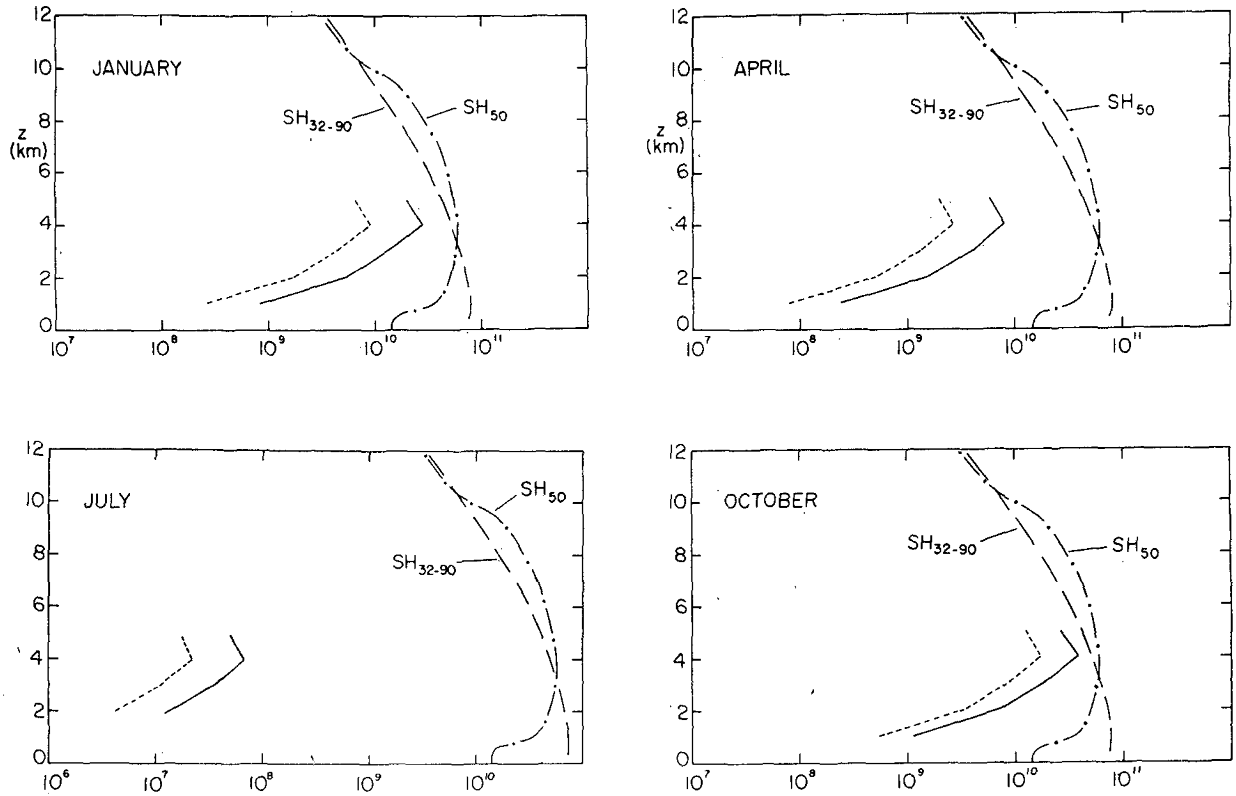


FIG. 7. Monthly values for upward transport of sensible heat at Tatoosh. Notation as in Fig. 1.

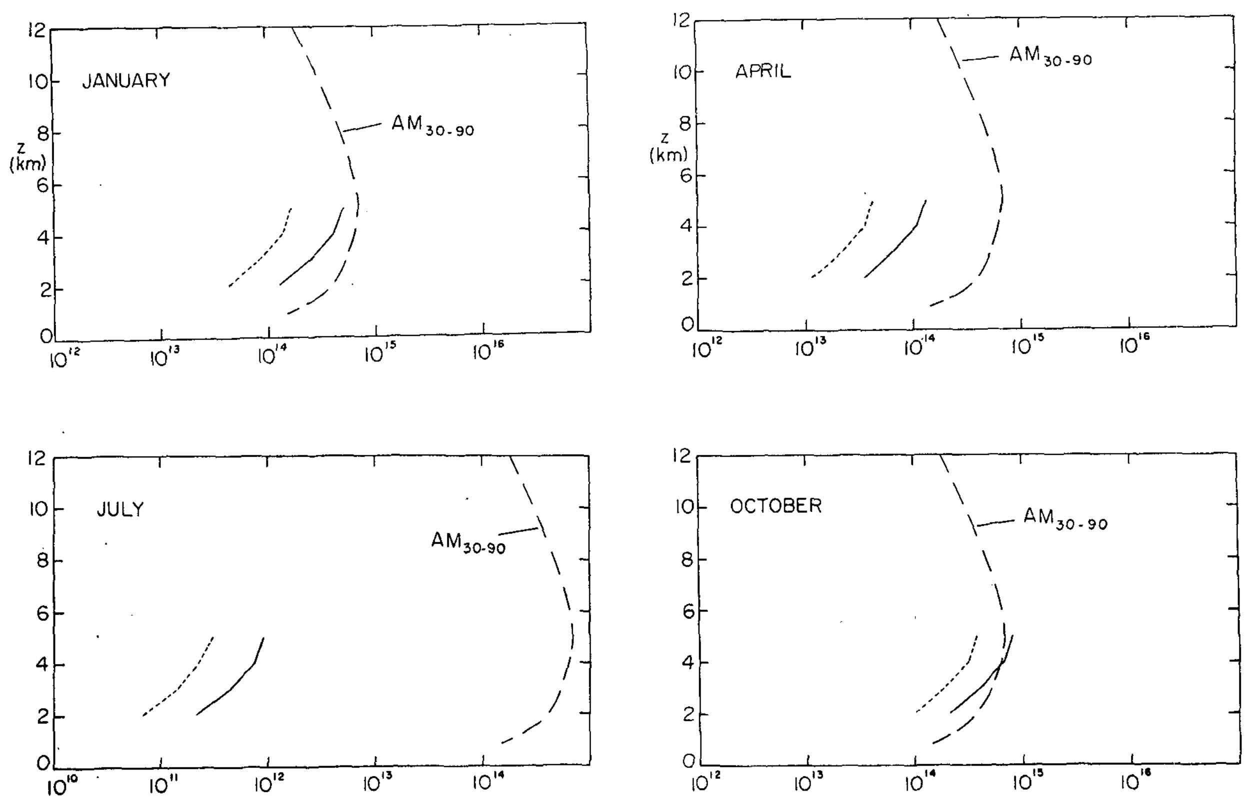


FIG. 8. Monthly values for downward transport of angular momentum at Tatoosh. Notation as in Fig. 2.

TABLE 3 Rainfall and wind shear statistics for stations and months in sample.

| Station | Month | Precipitation in sample: Cellular amount (cm) | Total amount (cm) | Number of hours | Hours of precipitation in typical month | Average shear during storms sampled ($m\ sec^{-1}\ km^{-1}$) |
|---|---|---|---|---|---|---|
| Boston | Jan. | 0.8 | 8.1 | 73 | 98 | 2.8 |
| | Apr. | 4.0 | 14.1 | 118 | 89 | 2.4 |
| | Jul. | 8.6 | 11.7 | 40 | 39 | 1.4 |
| | Oct. | 9.6 | 31.0 | 117 | 60 | 1.7 |
| Tatoosh | Jan. | 2.4 | 18.7 | 180 | 179 | 2.7 |
| | Apr. | 1.0 | 15.6 | 76 | 70 | 2.8 |
| | Jul. | 0.2 | 2.6 | 88 | 4 | 2.4 |
| | Oct. | 6.4 | 25.5 | 109 | 81 | 2.7 |
| San Juan | Jan. | 5.4 | 6.9 | 52 | 51 | 0.6 |
| | Apr. | 10.5 | 13.4 | 50 | 42 | 2.3 |
| | Jul. | 10.0 | 12.2 | 64 | 73 | 1.2 |
| | Oct. | 11.6 | 13.0 | 41 | 56 | 0.2 |
| New Orleans | Jan. | 5.2 | 18.2 | 94 | 38 | 4.8 |
| | Apr. | 16.2 | 19.9 | 32 | 32 | 2.5 |
| | Jul. | 8.2 | 9.4 | 23 | 47 | −0.1 |
| | Oct. | 2.4 | 4.4 | 17 | 26 | 1.3 |

Other factors as well as the presence of unstable maritime air influence the magnitude of the monthly transports. Some of them are indicated in Table 3, and it is of interest to note their interplay. For example, large transports are computed for a month such as January at Tatoosh (Figs. 7 and 8) which has a small percentage of cumulus-scale rainfall but a large number of hours of precipitation. A factor which strongly influences computed angular momentum transports is vertical wind shear. The reduction in momentum transport at New Orleans between April and July (Fig. 4) reflects the smaller shears associated with the summer convection more than a diminution of convective activity as compared with the spring storms. It should be noted that the small negative shear in July does not necessarily imply that the computed momentum transports should be upward since in the computations lifting and wind speeds were correlated hourly.

## 8. Comparison with larger scale fluxes

The relative significance of cumulus-scale vertical transports is judged by comparing them with larger scale vertical fluxes. From various studies it appears that the mean meridional transport is an important aspect of the angular momentum balance while synoptic-scale fluxes are a major factor in the heat budget. Therefore, these two types of larger scale fluxes are used for comparison. In addition, the cumulus heat transports are compared with estimates of the total required vertical eddy flux. This comparison is particularly relevant for San Juan since in the tropics neither mean meridional nor synoptic-scale vertical heat transports appear to be very large. The mean meridional transport of angular momentum and total required eddy transport of heat which are compared with cumulus fluxes are areal averages computed by Palmén and Newton (1969) for regions of the Northern Hemisphere north and south of latitude 30°. It should be noted that while all of Palmén and Newton's values are for winter conditions, their computations were the only ones of this type readily available. Synoptic-scale eddy fluxes of heat are obtained fron the numerical model calculations of Manabe *et al.* (1970).

Curves of the fluxes used for comparison are shown with the monthly cumulus transports in Figs. 1–8, and the comparisons are summarized in Table 4. It is immediately evident that during at least one season at each station, the cumulus-scale transports are of the same magnitude as some component of vertical flux which is generally recognized to be of significant magnitude. During other seasons the cumulus-scale values are often not especially large. Thus, while cumulus-scale heat and angular momentum transports may be rather minor under many circumstances, there are certain regions and seasons where these transports do become highly significant. In fact, they are probably more significant than Table 4 would indicate since the computations tend to underestimate the transports by failing to include the effects of downdrafts.

The regional and seasonal variability of cumulus-scale vertical transports points out the desirability of computing complete heat and angular momentum budgets for restricted areas of the globe. One such study has been carried out recently by Bunker (1971). If calculations of this type were available for various regions and seasons, more meaningful comparisons than are now possible could be made between cumulus and larger-scale fluxes.

Obviously the computed cumulus-scale transports are not accomplished evenly over an entire month, but only within periods of precipitation. Further, it was observed as the rain gauge data were processed that

TABLE 4. Summary of comparisons of monthly cumulus-scale transports with transports by circulations of other scales. Percentages refer to the size of computed cumulus-scale transports relative to estimated larger scale fluxes at the indicated heights and months and at the latitudes of the particular stations.

| Station | Type of transport | Comparative values for seasonal extremes | | Type of flux compared with and investigators from whom it was obtained | |
|---|---|---|---|---|---|
| | | Low | High | | |
| Boston | Heat | 10% at 4 km (Jan) | 70% at 6 km (Jul) | Synoptic-scale eddy at 40N | Manabe *et al.* (1970) |
| | Momentum | 15% at 4 km (Jan) | 100% above 6 km (Jul) | Mean meridional, high latitude | Palmén and Newton (1969) |
| Tatoosh | Heat | negligible (Jul) | 60% at 4 km (Oct) | Synoptic-scale eddy at 50N | Manabe *et al.* (1970) |
| | Momentum | negligible (Jul) | 120% at 5 km (Oct) | Mean meridional, high latitude | Palmén and Newton (1969) |
| San Juan | Heat | 20% at 2 km (Jan) | 100% at 7.5 km (Oct) | Total eddy (mean meridional not included) | Palmén and Newton (1969) |
| | Momentum | 25% at 3 km (Jan) | 100% at 9 km (Oct) | Mean meridional, low latitude | Palmén and Newton (1969) |
| New Orleans | Heat | 40% at 6.5 km (Jan) | 500% above 6 km (Apr & Jul) | Synoptic-scale eddy at 30N | Manabe *et al.* (1970) |
| | Momentum | 35% at 7 km (Jan) | 250% at 9 km (Apr) | Mean meridional, low latitude | Palmén and Newton (1969) |

two or three storms often contained large percentages of the total cellular rainfall for a month and the majority of the cumulus activity was concentrated within only a few hours. Thus, during certain periods, cumulus transports at a point are extremely large but remain zero most of the time.

## 9. Conclusions

The results of this study provide insight into the relative importance of cumulus-scale convection as a vertical transport mechanism in the atmosphere. The comparisons of computed cumulus-scale transports with transports by larger scales of motion show that cumulus transports become comparable in magnitude with important larger scale fluxes in climatologically predictable regions and seasons. At other times and places, cumulus-scale transports are much smaller, although not necessarily negligible. The role of cumulus as a transport mechanism is thus variable, occasionally quite important, and should be included in any complete consideration of atmospheric budgets of heat or angular momentum.

The basic premise of this study has been that much about the effect of cumuli on the larger scale atmosphere can be deduced from detailed precipitation measurements. An advantage of this procedure is that estimates of transports are based directly on measurements of cumulus activity rather than on residuals from measurements of larger scale quantities. The insight gained from the investigation is clear evidence of the usefulness of the approach.

*Acknowledgments.* Dr. Pauline M. Austin and Prof. James M. Austin provided the author with many helpful suggestions during this research. The work was sponsored by the National Science Foundation under Grant GA-10426.

APPENDIX

## Comparison of Model and Divergence Vertical Velocities

For 16 storms at Boston, the model storm vertical velocity $\bar{W}$ at level $\zeta$ was compared with vertical velocities deduced from horizontal divergence patterns. The technique of Bellamy (1949) was used to calculate the divergence over a triangular area surrounding Boston. Sounding data used in the computations were from Albany, N. Y., Portland, Me., and Nantucket, Mass., which are at the vertices of the triangle. "Model" and "triangle" vertical velocities are listed in Table A1. The values for the triangle are the maxima in the vertical distributions obtained at each observation time.

The following facts are noted from Table A1:

1) All of the storms are 6 hr or more in duration and are therefore considered to be of synoptic scale.

2) The negative vertical velocities obtained from the triangle in storms 6 and 7 occur when the fraction of the triangle covered by precipitation is small. These vertical velocities are therefore evidently not representative of their respective storms and may be ignored.

3) For all values of $\alpha$ and $\beta$, the model tends to overestimate the vertical velocity. The overestimate may be due in part to an adjustment which was made so that vertical velocities computed for the triangle were zero at the highest level for which winds were observed.

TABLE A1. Model storm-averaged vertical velocity $\bar{W}$ and vertical velocities $W_\Delta$ computed from horizontal divergence patterns by the triangulation method, in units of cm $\mathrm{sec}^{-1}$. Values in table are maxima in vertical profiles. Numbers in parentheses show percentage of wind triangle covered by precipitation at observation time. $\Delta t$ is the storm duration and $R_c$ the cellular precipitation.

| | | | | Model ($\bar{W}$) | | | | Triangle ($W_\Delta$) | | | |
|---|---|---|---|---|---|---|---|---|---|---|---|
| | | | | $\alpha$ | | | | Observation time | | | |
| Storm no. | $\Delta t$ (hr) | $R_c$ (inches) | $\beta$ | 0 | 0.33 | 0.67 | 1.00 | 1 | 2 | 3 | 4 |
| 1 | 30 | 2.75 | 1 | 34 | 38 | 41 | 45 | 15 | 18 | 15 | 13 |
| | | | 3 | 73 | 92 | 111 | 130 | (50%) | (100%) | (100%) | (75%) |
| 2 | 26 | 0.92 | 1 | 14 | 17 | 19 | 22 | 5 | 10 | 3 | |
| | | | 3 | 31 | 42 | 53 | 64 | (100%) | (100%) | (75%) | |
| 3 | 21 | 0.86 | 1 | 13 | 14 | 16 | 18 | 6 | 22 | | |
| | | | 3 | 31 | 38 | 45 | 52 | (5%) | (100%) | | |
| 4 | 14 | 0.52 | 1 | 13 | 14 | 14 | 16 | 13 | | | |
| | | | 3 | 31 | 34 | 38 | 41 | (30%) | | | |
| 5 | 27 | 0.40 | 1 | 17 | 18 | 20 | 22 | 13 | 8 | | |
| | | | 3 | 27 | 36 | 47 | 57 | (100%) | (50%) | | |
| 6 | 11 | 0.36 | 1 | 14 | 15 | 16 | 17 | −4 | | | |
| | | | 3 | 30 | 36 | 43 | 50 | (25%) | | | |
| 7 | 26 | 0.32 | 1 | 7 | 8 | 9 | 10 | −16 | −14 | | |
| | | | 3 | 12 | 17 | 21 | 26 | (20%) | (30%) | | |
| 8 | 7 | 0.32 | 1 | 12 | 13 | 13 | 14 | 7 | | | |
| | | | 3 | 31 | 34 | 37 | 40 | (85%) | | | |
| 9 | 30 | 0.21 | 1 | 8 | 9 | 9 | 10 | 13 | 23 | | |
| | | | 3 | 11 | 15 | 19 | 24 | (75%) | (100%) | | |
| 10 | 6 | 0.21 | 1 | 21 | 21 | 21 | 21 | 14 | | | |
| | | | 3 | 40 | 40 | 40 | 40 | (100%) | | | |
| 11 | 36 | 0.16 | 1 | 14 | 15 | 16 | 16 | 11 | 14 | 12 | 5 |
| | | | 3 | 16 | 23 | 31 | 39 | (50%) | (100%) | (100%) | (30%) |
| 12 | 29 | 0.12 | 1 | 4 | 6 | 9 | 11 | 1 | 5 | | |
| | | | 3 | 7 | 15 | 23 | 31 | (25%) | (not determined) | | |
| 13 | 7 | 0.12 | 1 | 13 | 16 | 18 | 20 | 3 | | | |
| | | | 3 | 21 | 33 | 45 | 56 | (75%) | | | |
| 14 | 18 | 0.11 | 1 | 5 | 5 | 6 | 6 | 6 | 5 | | |
| | | | 3 | 9 | 10 | 11 | 12 | (100%) | (100%) | | |
| 15 | 24 | 0.11 | 1 | 12 | 13 | 23 | 28 | 7 | 7 | 14 | |
| | | | 3 | 16 | 35 | 55 | 75 | (50%) | (50%) | (75%) | |
| 16 | 9 | 0.10 | 1 | 5 | 5 | 5 | 6 | 8 | | | |
| | | | 3 | 7 | 9 | 11 | 13 | (50%) | | | |

4) For $\beta=1$, agreement between model and triangle values is within a factor of 2, for at least one value of $\alpha$ and at least one sounding time in each storm except 13.

5) For $\beta=3$ and $\alpha=0.67$ or 1.00, the model and triangle values are not in agreement. The model vertical velocities are larger by a factor of 4 or more in half of the storms.

The significant finding of those listed above is that the model tends to overestimate highly the storm-averaged vertical velocity for combinations of large $\alpha$ with large $\beta$. This result is consistent with qualitative reasoning which suggests that when cumulus cells are embedded in a synoptic-scale precipitation area, the condensate which they leave aloft is rained out at some time and place within the larger scale storm.

## REFERENCES


Austin, P. M., and R. A. Houze, Jr., 1972: Analysis of the structure of precipitation patterns in New England. *J. Appl. Meteor.*, **11**, 926–935.

——, and ——, 1973: A technique for computing vertical transports by precipitating cumuli. *J. Atmos. Sci.*, **30**, 1100–1111.

Bellamy, J. C., 1949: Objective calculations of divergence, vertical velocity, and vorticity. *Bull. Amer. Meteor. Soc.*, **30**, 45–49.

Bunker, A. F., 1971: Energy transfer and tropical cell structure over the central Pacific. *J. Atmos. Sci.*, **28**, 1101–1116.

Manabe, S., J. Smagorinsky, J. L. Holloway, Jr., and H. M. Stone, 1970: Simulated climatology of a general circulation model with a hydrologic cycle III. Effects of increased horizontal computational resolution. *Mon. Wea. Rev.*, **98**, 175–213.

Palmén, E., and C. W. Newton, 1969: *Atmospheric Circulation Systems*. New York, Academic Press, 603 pp.

Smagorinsky, J., S. Manabe and J. L. Holloway, Jr., 1965: Numerical results from a nine-level general circulation model of the atmosphere. *Mon. Wea. Rev.*, **93**, 727–768.

Starr, V. P., and R. M. White, 1954: Balance requirements of the general circulation. Geophys. Res. Papers, No. 35, Air Force Cambridge Research Center, 57 pp.